www.czasopisma.pan.pl PAN www.journals.pan.pl

Acta Geologica Polonica, Vol. 68 (2018), No. 4, pp. 689–709
DOI: 10.1515/agp-2018-0037

New data on the continental deposits from the Cao Bang Basin (Cao Bang-Tien Yen Fault Zone, NE Vietnam) – biostratigraphy, provenance and facies pattern

ANNA WYSOCKA[1*], PHAN DONG PHA[2, 3*], EWA DURSKA[1], URSZULA CZARNIECKA[4], DO VAN THANG[1, 2], ANNA FILIPEK[1], NGUYEN QUOC CUONG[5], DANG MINH TUAN[3, 5], NGUYEN XUAN HUYEN[5] and HOANG VAN THA[5]

[1] *Faculty of Geology, University of Warsaw, Żwirki i Wigury 93, PL-02-089, Warsaw, Poland. E-mail: anna.wysocka@uw.edu.pl*
[2] *Institute of Marine Geology and Geophysics, Vietnam Academy of Science and Technology, Building A27, 18 Hoang Quoc Viet Str., Cau Giay Distr., Hanoi, Vietnam. E-mail: phandongpha@gmail.com*
[3] *Graduate University of Science and Technology, Vietnam Academy of Science and Technology, Building A21, 18 Hoang Quoc Viet Str., CauGiay Distr., Hanoi, Vietnam.*
[4] *Department of Geosciences, University of Oslo, P.O Box 1047 Blindern, 0316 Oslo, Norway.*
[5] *Institute of Geological Sciences, Vietnam Academy of Science and Technology, 84 Chua Lang Str., Dong Da Distr., Hanoi, Vietnam.*
** corresponding authors*

ABSTRACT:

Wysocka, A., Pha, D.P., Durska E., Czarniecka, U., Thang, D.V., Filipek A., Cuong, N.Q., Tuan, D.M., Huyen, N.X. and Tha, H.V. 2018. New data on the continental deposits from the Cao Bang Basin (Cao Bang-Tien Yen Fault Zone, NE Vietnam) – biostratigraphy, provenance and facies pattern. *Acta Geologica Polonica*, **68** (4), 689–709. Warszawa.

The Cao Bang Basin is the northernmost of the basins related to the Cao Bang-Tien Yen Fault Zone in northern Vietnam. The basin is filled with a thick series of continental deposits. However, the exact age of the sedimentary basin infill has been under discussion for a long time. Because of new published data, the authors have decided to revisit this basin. Palynological data has allowed us to assign the Cao Bang Basin infill to the Lower Oligocene PC1 complex of the Shangcun Fm. (southern China). Among the saccate grains of gymnosperms, the domination of *Cathaya* and *Pinus* was observed, whereas angiosperms are represented by *Carya*, *Celtis*, Hammamelidaceae, *Ulmus* and also *Pterocarya*, *Quercus*, the *Castanea–Castanopsis–Lithocarpus* group, and the Loranthaceae. Among pteridophytes occur *Laevigatosporites*, Osmundaceae, and *Pteris*. The sedimentological features of the Cao Bang Basin are distinct from those of other basins from the Cao Bang-Tien Yen Fault Zone. The basin is filled with a wide variety of clastic deposits, from some of coarse-grained, alluvial-fan origin, through sandy beds of fluvial origin up to fine, organic-rich lacustrine deposits. The coarse-grained lithofacies are built of clasts derived mainly from local sources. The sandstones from the basin equally are submature or immature. They contain a lot of lithoclasts, the composition of which depends on the sample location within the basin. The potential source area is composed of older sedimentary units and of granitic rocks. The geochemical samples studied reflect the geochemical composition of silicic source rocks with only a minor contribution of basic components. The succession that fills the basin is interpreted as a typical fill for relatively long-lasting evolving half-graben or strike-slip basins. Moreover, the basin is partly occupied by a subsequent present-day sedimentary basin of Quaternary age.

Key words: Continental environments; Pollen and spores; Provenance; Palaeogene; Cao Bang; Vietnam.

INTRODUCTION

The Cao Bang Basin (CBB) is the northernmost of the basins related to the Cao Bang-Tien Yen Fault Zone (CB-TY FZ) (Text-fig. 1B). Its basement is built of various Mesozoic and Palaeozoic sedimentary and magmatic rocks (e.g., Triassic granites, peridotites and gabbro, as well as Permian basalts and tuffs) (Text-fig. 2). The basin is NW-SE elongated and directly limited by two fault lines and, as suggested by Pubellier *et al.* (2003), had a polyphase evolution with a large component of extension and evolved as a sigmoid pull-apart basin.

Previously Wysocka *et al.* (2009) distinguished the CBB as one of the alluvial-to-lacustrine basin type. Moreover, the origin of the accommodation space in the CBB was linked with an early to middle Miocene sinistral transtensional regime along the CB-TY FZ. Such a tectonic setting was thought to have caused complex changes both in the lateral and vertical displacement through time. Consequently, the other basins related to the CB-TY FZ, including the CBB, were treated as diachronic, reflecting complex unconformities. The post-depositional uplift, the tectonic deformations, and the pre-Quaternary erosion in the studied basins were correlated with a sinistral transpressional regime.

However, the above interpretation on the origin and evolution of the CBB was highly speculative because of the lack of knowledge of the exact stratigraphic position of the deposits that filled the CBB. Recently, we have decided to revisit the CBB because of new regional biostratigraphical data published e.g., by Böhme *et al.* (2011, 2013), Neubauer *et al.* (2012), Ducroq *et al.* (2015) and Prieto *et al.* (2017).

The discussion on the age of the deposits from the basins related to the CB-TY FZ has continued over many years. Based on the general geological map (Thuy 2000), the CBB is filled with deposits that belong to the upper Miocene Na Duong Fm. However, based on the detailed geological map, they are of the middle Miocene age and belong to the Cao Bang Formation (Tran and Trinh 1975; Cuong *et al.* 2000). Moreover, in some recent papers and books deposits from the basins related to the CB-TY FZ, included the Cao Bang, Na Duong and Rinh Chua formations, are ascribed to the Eocene–Oligocene (Böhme *et al.* 2011, 2013; Ducroq *et al.* 2015), Eocene–Neogene (Hoang *et al.* 2004), Oligocene–Miocene (Prieto *et al.* 2017) or even Eocene–Miocene (Tri and Khuc 2011). Most of the studies mentioned above were based mainly on mammals, gastropods, bivalves, fishes and turtles, therefore we have decided to focus on palynomorphs. Moreover, we have decided to extend our investigation of the petrography into a more detailed provenance study. As a result, the CBB was revisited in 2016 and 2017.

GEOLOGIC OVERVIEW

North-eastern Vietnam is a classic area of structural and geotectonic interest. One of the most important topics in this field is the Cenozoic movement along the Red River Fault Zone (RRFZ), the main strike-slip zone of SE Asia, which separates the South China and the Indochina terranes (Text-fig. 1A). Left-lateral shearing along the RRFZ is dated as Oligocene and Miocene (Leloup *et al.* 1995, 2001) with estimates of the left-lateral offsets between 300 and 700 km (Tapponnier *et al.* 1986, 1990). However, the offset for the RRFZ in the area of the Tonkin Gulf probably does not exceed a few tens of kilometres (Rangin *et al.* 1995; Morley 2002, 2007). At present, this zone corresponds to right-lateral movements which started about 5.5 Ma (e.g., Allen *et al.* 1984; Tapponnier *et al.* 1990; Leloup *et al.* 1995; Fyhn and Phach 2015).

The CB-TY FZ is located about 150 km northeast of the RRFZ (Text-fig. 1). This zone is only vaguely known; so far, only a few studies have been devoted to its structural setting (Chinh 2000; Pubellier *et al.* 2003; Cuong *et al.* 2006; Fyhn *et al.* 2018), with only some maps (Cuong *et al.* 2000; Thuy 2000; Binh *et al.* 2003; Hoang *et al.* 2004), a few sedimentological interpretations (Wysocka *et al.* 2005, 2006; Gmur 2006; Wysocka 2009; Böhme *et al.* 2013) and some diversified stratigraphic schemes being published (Tran and Trinh 1975; Trinh 1979; Pham, 2000; Trung *et al.* 2000; Thuan 2006; Böhme *et al.* 2011, 2013; Ducroq *et al.* 2015).

The CBB is the northernmost of the basins related to the CB-TY FZ (Text-figs 1B and 2). Its basement is built of various Mesozoic and Palaeozoic sedimentary rocks (conglomerates, sandstones, siltstones and limestones) and magmatic rocks (Triassic granites, peridotites and gabbros, as well as Permian basalts and tuffs; Text-fig. 2). The basin is NW-SE elongated and filled with a thick sequence of clastic rocks, resting unconformably on basement rocks, dipping slightly, mostly to the northeast. The LK1 borehole (for location see Text-fig. 2) suggests a thickness of basin infill of about 150 m. However, because of the tilting, the stratigraphic thickness of the basin infill could be larger. At present, the basin is bordered by two fault lines and partly occupied by a subsequent Quaternary sedimentary basin (Text-fig. 2).

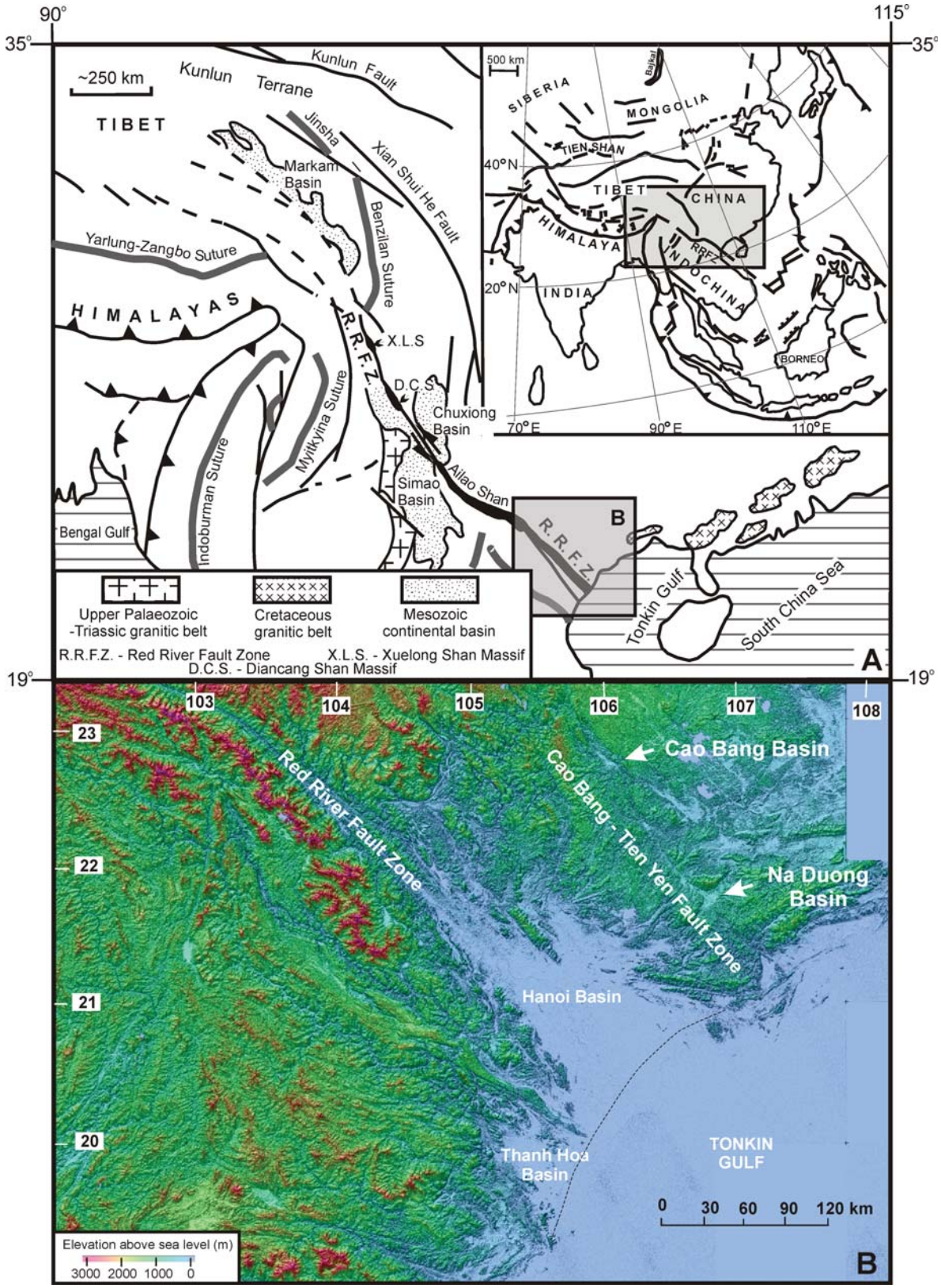

Text-fig. 1. A – Tectonic sketch-map of SE Asia (based on Tapponnier *et al*. 1986). B – Geological structures of northern Vietnam related to the studied Cao Bang Basin on a DEM (SRTM) image

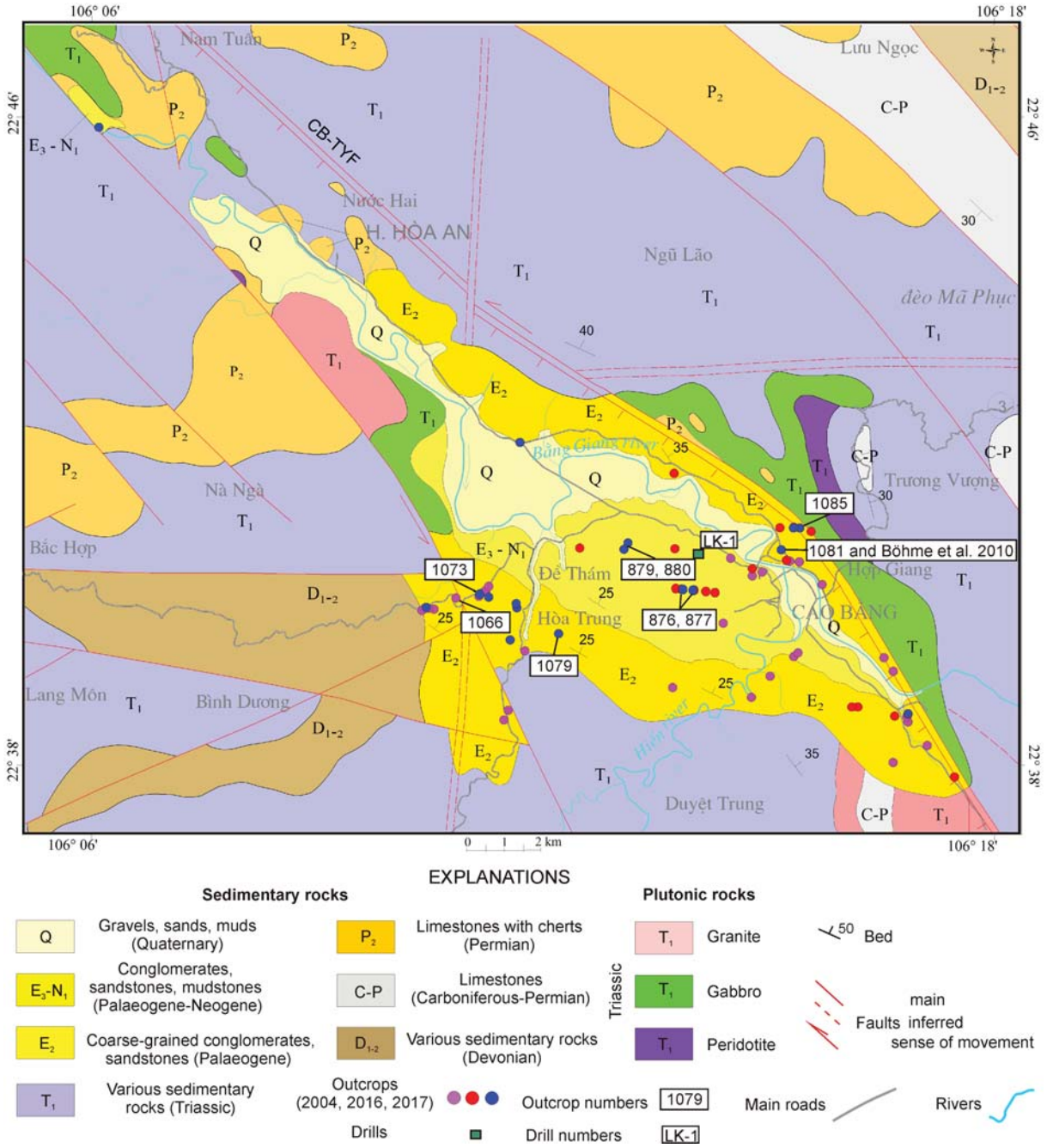

Text-fig. 2. Geological map of the Cao Bang Basin and adjacent areas (compilation based on maps by Cuong *et al.* 2000; Binh *et al.* 2003; Hoang *et al.* 2004; Hung *et al.* 2007 and Lan *et al.* 2011)

The CBB is filled with a broad variety of clastic deposits: sand- and mud-supported disorganised conglomerates (G), massive or amalgamated bodies of conglomerates (Gmm), sand- and mud-supported crudely stratified conglomerates (Gmg), planar and trough cross-stratified sand-supported conglomerates (Gp/Gt), massive or amalgamated beds of sandstones (Sm), planar and trough cross-stratified sandstones (Sp/St), ripple cross-laminated sandstones (Sr), horizontal-laminated sandstones (Sh), horizontal-laminated fine sandstones and siltstones, occasionally with normal grading (Sng), massive siltstones (Fsm),

Depositional environment	Lithofacies	Description	Interpretation
Alluvial fan	Sand- and mud-supported disorganised conglomerates (G)	Decimetre thick; poorly defined, discontinuous beds; pebble-size and well-rounded clasts; sand to mud matrix.	Deposition from gravity and/or high-concentration flow.
	Massive or amalgamated bodies of conglomerates (Gmm)	Up to several metres thick; highly amalgamated; cobble- to pebble-size and angular to sub-rounded clasts; clast- to sand-supported; undefined base and top.	Deposition from high-concentration flow.
Gravel-dominated fluvial channel	Sand- and mud-supported crudely stratified conglomerates (Gmg)	Up to several metres thick; highly amalgamated; pebble- to cobble-size and angular to sub-rounded clasts; sand- to mud matrix; may be erosively based.	Deposition from high-concentration flow.
	Planar and trough cross-stratified sand-supported conglomerates (Gp/Gt)	Up to 3 metres thick; highly amalgamated; planar or low angle trough cross-stratified; pebble-size and sub-rounded to well-rounded clasts; gravel patches with partly open-work fabric common; fining-up trend; very coarse to coarse sand matrix; erosively based.	Bedload transport; downstream migration of sinuous-crested barforms.
Sand-dominated fluvial channel	Massive or amalgamated beds of sandstones (Sm)	Up to several metres thick; poorly defined beds; poorly sorted; isolated pebbly sandstone lenticles and layers; occasionally normally graded; often developed above the Gt litofacies as part of a fining-up trend.	Upper plane bed flow.
	Planar and trough cross-stratified sandstones (Sp/St)	Variable thickness of sets; poorly to well sorted; medium to coarse grained; low angle bounding surfaces; occasionally coalified flora fragments, and muddy intraclasts.	Downstream migration of ripple and dune scale sinuous- (St) or straight-crested (Sp) barforms, in some cases falling to low stage gravelly barform modifications.
Flood plain/lake	Ripple cross-laminated sandstones (Sr)	Thin sets; well sorted; fine-grained; asymmetric straight or sinuous ripples.	Downstream migration of small-scale current ripples.
	Horizontal-laminated sandstones (Sh)	Horizontally laminated fine sandstones; occasionally beds with coalified flora detritus, with rare molluscs.	Deposition from currents gradually decreasing in velocity.
	Massive siltstones (Fsm)	Generally thick (a few metres); massive or poorly stratified; commonly alternated with sandy siltstones; occasionally pedogenic structures.	Deposition of fine grains from currents of low velocity and/or from suspension, occasionally subaerial conditions.
	Laminated siltstones (Fl)	Thick series of stratified siltstones, with mollusc shells and coalified flora detritus.	Deposition of suspended material.
	Coaly claystones (FC)	Generally thick series (a few metres); poorly stratified; alternated with siltstone beds; occasionally with the coal layers.	Phytogenic accumulation with a high supply of clastic material.

Table 1. Depositional environments in the studied sequence of the Cao Bang Basin based on lithofacies characteristics

laminated siltstones (Fl), and coaly claystones (FC) (Table 1). They represent variable continental depositional environments such as alluvial fan, fluvial and lacustrine (Wysocka 2009).

MATERIAL AND METHODS

The studied deposits can be traced along the cuttings of new roads under construction, in brick factories, and in open sand and gravel pits. Observations from 17 outcrops in 2017 were added to the observations that had been done before (for outcrop location see Text-fig. 2). In total, the observations from about fifty geological sites were interpreted, and detailed sections and analyses were done for nine outcrops (for GPS coordinates see Table 2). Based on the dominant grain-size class, texture, stratification, degree of clast rounding and sorting, eleven lithofacies were recognised following the concept of Miall (1977, 1978).

Outcrop number	Outcrop GPS coordinates
876	22°40’6.30”N; 106°13’50.30”E
877	22°40’4.50”N; 106°14’4.00”E
879	22°40’36.20”N; 106°13’6.30”E
880	22°40’41.90”N; 106°13’10.10”E
1066	22°39’54.80”N; 106°10’27.30”E
1073	22°40’5.78”N; 106°11’11.07”E
1079	22°39’33.90”N; 106°12’18.90”E
1081	22°40’35.00”N; 106°15’11.50”E
1085	22°40’50.80”N; 106°15’20.70”E

Table 2. GPS coordinates for the investigated outcrops

The depositional mechanisms were interpreted and assigned to lithofacies (Table 1). The lithofacies were grouped into facies associations representing distinct depositional environments (Table 1). Samples of siltstone, medium- and fine-grained sandstone and conglomerate were collected for standard palynological, petrographical and geochemical analysis.

Palynological analyses were carried out on ten samples from outcrops located in the central part of the CBB. The samples were washed under running water, then a 30% HF solution was added to dissolve the silica. The residuum was sieved on a 10 µm sieve. $ZnCl_2$ was used to separate undissolved mineral particles and organic matter. The slides were made with glycerine jelly as a mounting medium. At least 150 sporomorphs were counted in each sample.

Petrographic and geochemical analyses were processed on the samples from outcrops: 876, 877, 880, 1073, 1079 and 1085 (for location see Text-fig. 2). In total seven samples were analysed for petrographic data, and four for bulk-rock geochemistry.

Petrographic investigations of clastic rocks were performed on 7 standard uncovered polished thin sections using a polarising microscope. Sandstones were chosen for further analysis. Framework composition, matrix and cements were quantified. Furthermore, the size of the framework components was examined. The studied deposits were classified based on the classification scheme of fine-grained sedimentary rocks (Picard 1971), whereas sorting of the framework components was determined using comparison charts (Longiaru 1987). In general, the sandstones were classified using combined ternary petrographic classification schemes (McBride 1963; Dott Jr 1964; Folk *et al*. 1970; Pettijohn *et al*. 1972; Williams *et al*. 1982). Quantitative petrographic information and description of the most important textural features are listed in Appendix 1.

Preliminary whole-rock geochemical analysis was conducted on 4 samples. The oxides of major elements, trace and rare earth elements were determined by laser ablation inductively coupled plasma mass spectrometry (LA-ICP-MS) at the Bureau Veritas Minerals Laboratories Ltd. in Vancouver, Canada. The results of these analyses are provided in Appendix 2.

RESULTS

Palynomorphs

The palynomorphs are present only in five samples studied, from outcrops 879 and 880 (for location see Text-fig. 2). In four samples their frequency was high enough to perform a palynological analysis (Table 3). The palynological spectra are taxonomically poorly diversified and the sporomorphs are not abundant. For example, two slides were used to count 150 sporomorphs in sample 879 (3).

In four analysed samples: 879 (2), 879 (3) 880 (1), and 880 (3), the saccate gymnosperm pollen (*Pinuspollenites* and *Cathaypollis*) plays the most important role. It constitutes from 29.4% in sample 880 (1) to as much as 64.5% in sample 879 (3) (Table 3). Other frequent pollen grains include (Table 3): *Caryapollenites* (0–5.9%) (Text-fig. 3C), *Celtispollenites* (0–13.8%) (Text-fig. 3E), *Cupuliferoipollenites oviformis–C. pusillus* (0–5.7%) (Text-fig. 3I), Hammamelidaceae-type (0–3.5%) (Text-fig. 3F), Loranthaceae-type (0–17.8%) (Text-fig. 3G–H), *Quercoipollenites–Quercoidites* (0–4.1%) (Text-fig. 3J), *Sapotaceae*-type (0–4.6%), and *Ulmipollenites* (0–1.3%) (Text-fig. 3B). In some samples cryptogams are quite frequent, e.g., *Baculatisporites* (0.6–29.5%) (Text-fig. 3K) and *Polypodiaceoisporites* (0–5.3%) (Text-fig. 3L).

The difficulty in determining the precise age of the palynofloras of Palaeogene/Neogene age, such as the one from Cao Bang, lies in the fact that their taxonomical composition is similar in general aspects. Usually it lacks index fossils and the differences found concern, for instance, percentages of some types of pollen or the number of taxa characteristic of tropical/subtropical climate *vs*. temperate climate. Thus, the only way to specify the age of the investigated CBB palynoflora was by comparing it to other fossil pollen and spores assemblages of known age from nearby areas (namely Southern China).

The middle Eocene palynoflora described from the Changchang Formation (Hainan Island, China) is dominated by angiosperm pollen (Yao *et al*. 2009; Spicer *et al*. 2014). Prevailing are tricolpate and tricolporoidate grains of *Faguspollenites*, *Cupuliferoipollenites*, *Quercoidites*, and *Castanopsis* (these taxa constitute almost 90%). The tropical and subtropical element is represented by such pollen as *Proteacidites*, *Myrtaceidites* and *Ephedripites* (Yao *et al*. 2009). The middle and late Eocene palynological assemblages from the Maoming Basin: Youganwo and Huangniuling formations (Guangdong Province, Southern China) are dominated by spores and angiosperms pollen represented mostly by small tricolpate grains such as *Quercoidites*, *Quercus gracilis*, *Q. graciliformis*, *Tricolporopollenites* (*T. cingulum*, *T. liblarensis*); porate grains like *Alnipollenites*, *Ulmaceae* and others are also frequent (Alexandrova *et al*. 2015).

Morphological name	Nearest living relative	Samples			
		879(2)	879(3)	880(1)	880(3)
Alnipollenites Potonié, 1931	*Alnus*	1.1	0.0	0.0	0.0
Baculatisporites Pflug and Thomson in Thomson and Pflug, 1953	*Osmunda*	4.6	0.7	0.6	29.5
Carpinipites Srivastava, 1966	*Carpinus*	0.0	0.0	1.8	0.0
Caryapollenites Raatz,1937	*Carya*	3.4	5.9	7.6	1.4
Cathayapollis Ziembińska-Tworzydło, 2009	*Cathaya*	19.5	29.6	7.6	22.7
Celtispollenites Nagy, 1969	*Celtis*	13.8	0.0	7.6	0.0
Corsinipollenites Nakoman, 1965	Onagraceae	0.0	0.0	0.6	0.0
Cupuliferoipollenites ovformis C. pusillus (Potonié, 1934) Potonié, 1951	*Castanea–Castanopsis–Lithocarpus*	5.7	0.0	0.6	0.0
Foveotriletes Potonié, 1956	?	0.0	0.0	0.0	0.5
Hammamelidaceae-type	Hamamelidaceae	0.0	0.7	3.5	0.0
Laevigatosporites Ibrahim, 1933	many cryptogams families	1.1	5.3	34.1	6.8
Leiotriletes (Naumova, 1937) Potonié and Kremp, 1954	Lygodiaceae	0,0	0.0	0.0	0.0
Loranthaceae-type	Loranthaceae	0.0	17.8	0.0	0.0
Microfoveolatisporis Krutzsch, 1959	Schizaceae	0.0	0.0	0.0	0.0
Momipites Wodehouse, 1933	*Engelhardia*	1.1	0.0	0.0	0.0
Periporopollenites Pflug and Thomson in Thomson and Pflug, 1953	*Liquidambar*	0.0	0.0	2.4	0.0
Persicarioipollis Krutzsch, 1962	Polygonaceae	1.1	0.0	0.0	0.0
Piceapollis Krutzsch, 1971	*Picea*	0.0	0.0	2.4	0.0
Pinuspollenites Raatz, 1937	*Pinus*	18.4	34.9	21.8	30.4
Platycaryapollenites Nagy, 1969	*Platycarya*	2.3	0.0	0.6	0.0
Polyatriopollenites Pflug, 1953 in Thomson and Pflug, 1953	*Pterocarya*	1.1	0.7	0.0	0.5
Polypodiaceoisporites Potonié, 1951	*Pteris*	0.0	3.3	0.6	5.3
Quercopollenites Nagy, 1969	*Quercus*	1.1	0.0	4.1	0.0
Quercoidites Potonié, Thomson and Thiergart, 1950					
Retitriletes Pierce, 1961	*Lycopodium*	0.0	0.0	0.0	0.5
Salixpollenites Srivastava, 1966	*Salix*	0.0	0.0	1.8	0.0
Sapotaceae-type	Sapotaceae	4.6	0.0	0.0	0.0
Sciadopityspollenites Raatz, 1937	*Sciadopitys*	0.0	0.0	0.6	0.0
Slovakipollis Krutzsch, 1962	Eleagnaceae	0.0	0.0	0.0	1.0
Stereisporites Pflug in Thomson and Pflug, 1953	*Sphagnum*	0.0	0.0	1.2	0.0
Ulmipollenites Wolff, 1934	*Ulmus*	0.0	1.3	0.6	0.0
Verrucatosporites Pflug and Thomson in Thomson and Pflug, 1953	*Davalia*	0.0	0.0	0.0	1.4
Unknown porate pollen		20.7	0.0	0.0	0.0

Table 3. Percentages of palynomorphs found in the studied samples

Early Oligocene palynofloras are known from the Maoming Basin Shangcun Formation (Guangdong Province, South China) (Herman *et al*. 2017). Three palynological complexes are described here: the PC1 complex is characterised by a predominance of gymnosperms (over 70%), representing mostly the Pinaceae and the Taxodiaceae–Cupressaceae families. Among angiosperms there dominate *Corylopsis*, *Liquidambar*, *Hammamelis*, *Carya*, *Quercus* and Fagaceae. Angiosperm pollen (over 60%) prevails in the overlying PC2 and PC3 complexes; it is represented mainly by *Quercus*, and the *Castanea–Castanopsis* and *Rhoipites–Fususpollenites* groups.

The studied CBB palynoflora is taxonomically poorly diversified. Among the most frequent are saccate grains of gymnosperms, mainly *Cathayapollis* and *Pinuspollenites*. They constitute 30–50% of all grains in the spectra. Among the angiosperms there prevail *Carya*, *Celtis*, Hammamelidaceae, *Ulmus* and also the Loranthaceae, *Pterocarya*, *Quercus*, and the *Castanea–Castanopsis–Lithocarpus* group. Among the pteridophytes *Laevigatosporites*, *Osmundaceae*, and *Pteris* occur frequently in some samples. Most of the taxa present represent a warm temperate climate. Subtropical and tropical taxa like the Sapotaceae and the Loranthaceae occur occasionally. In general terms the composition of the assemblage corresponds well with the lower part of the lower Oligocene

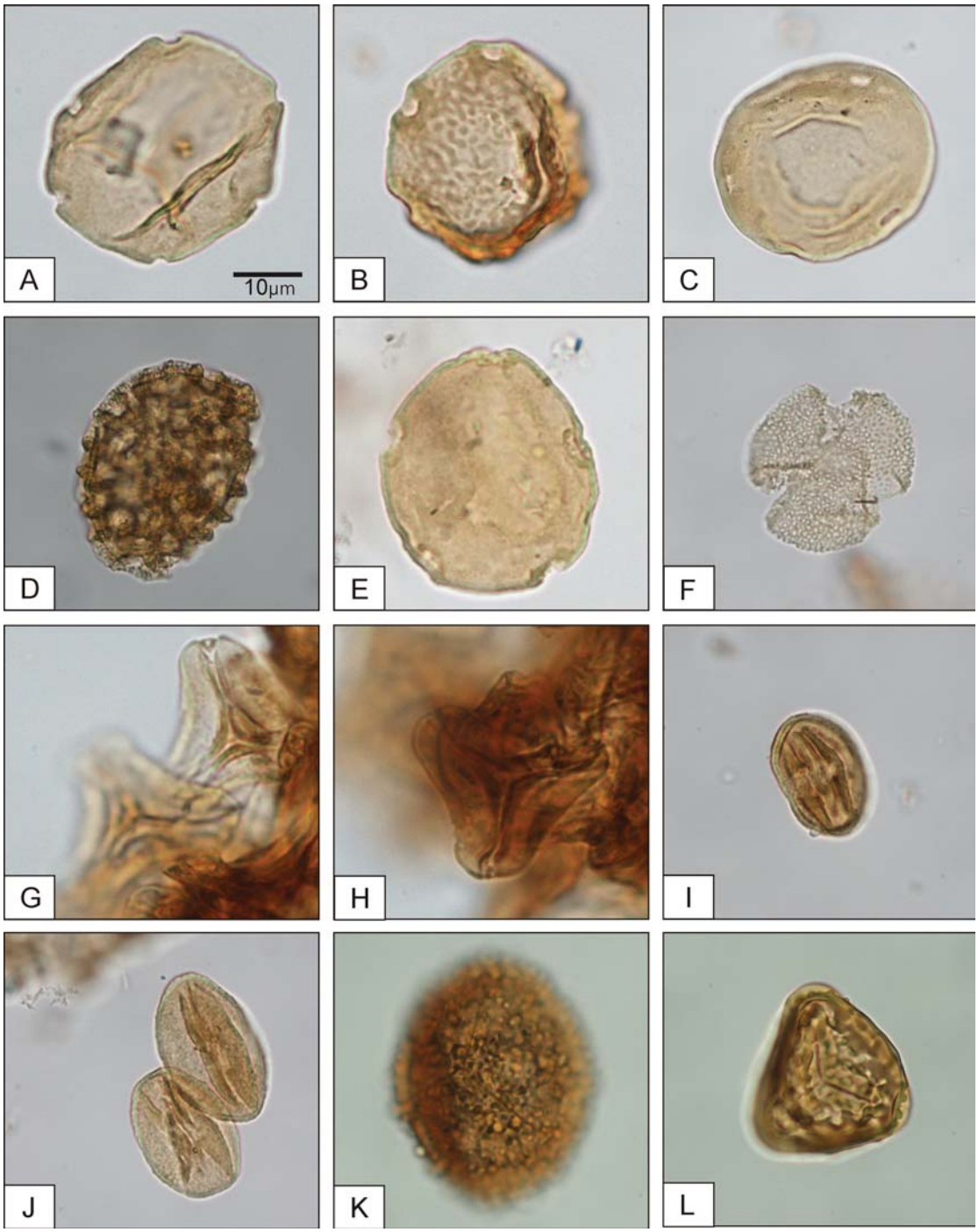

Text-fig. 3. Microphotographs of the identified palynomorphs. **A** – *Polyatriopollenites*; **B** – *Ulmipollis*; **C** – *Caryapollenites*; **D** – *Persicarioipollis*; **E** – *Celtispollenites*; **F** – Hammamelidaceae – type; **G, H** – Loranthaceae-type; **I** – *Cupuliferoipollenites*; **J** – *Quercopollenites*; **K** – *Baculatisporites*; **L** – *Polypodiaceoisporites*

PC1 complex of the Shangcun Formation outlined above (Herman *et al.* 2017). Common for both palynofloras are: dominance of gymnosperm pollen and significant abundance of *Carya*, *Liquidambar*, Hammamelidaceae, and *Quercus* pollen. According to Herman et al. (2017 and references therein) the palynofloras of the lower part of the lower Oligocene are characterised by the predominance of Pinaceae

pollen, and an impoverishment in the angiosperm pollen taxa. Such a condition is explained by these authors as a result of the disappearance of most of the subtropical and tropical taxa, in comparison to the Eocene assemblages. If the CBB sediments were older (e.g., of Eocene age), *Quercoidites* and *Quercopollenites* as well as other small tricolporate grains should play a key role in the spectra (Ye *et al*. 1996; Yao *et al*. 2009; Alexandrova *et al*. 2015). Also more taxa characteristic of tropical and subtropical climates should be present. If the assemblage was of late early or late Oligocene age, likewise more subtropical and tropical taxa would be present which is observed for the palynofloras of this age (Herman *et al*. 2017). Another indicator allowing us to determine the age of the CBB fossil flora is the presence of *Persicarioipollis*. Although only one pollen grain of this taxon was found in the samples studied (Text-fig. 3D), its presence also points to the Oligocene as it is not known from older sediments in SE Asia (Shaw 1998; Yi *et al*. 2003; Herman *et al*. 2017).

Ye *et al*. (1996) proposed sporopollen assemblages typical of the Palaeogene and Neogene of China. An indicated by these authors, the South China Sporopollen Region includes Guangxi, Yunnan, Guangdong and the South China Sea area, thus lying in the vicinity of the Cao Bang Basin. The *Quercoidites microhenrici*–Pteridophyta spores–*Alnipollenites* Sporopollen Assemblage is suggested as being typical of the Eocene. It is characterised till its latest stage by the dominance of tricolpate pollen and thus, as mentioned above, does not match the studied fossil flora. The Oligocene assemblage zone is the *Magnastriatites howardi–Quercoidites–Gothanipollis* Assemblage. Although *Quercoidites* pollen is still indicated as a dominant element, other taxa, which are also frequent in the CBB succession, are abundant in this zone and include: *Momipites* (*Engelhardia*), *Gothanipollis* (Loranthaceae), *Periporopollenites* (*Liquidambar*), *Cupuliferoipollenites*, and *Caryapollenites*. *Persicarioipollis* appears in this sporopollen assemblage in small amounts. Thus this assemblage, although not fitting perfectly, seems to be more applicable than the Eocene one.

The interpretation based on published Vietnamese maps showing the Neogene (Miocene) age of the CBB does not seem to be realistic in the light of palynologic data. In the Miocene, *Betula*, Chenopodiaceae, and Graminae pollen play an important role in the pollen spectra of south-eastern China (Ye *et al*. 1996; Wang 2006). Assignment of the CBB sediments to the early Oligocene is in accordance with the results of Böhme *et al*. (2011).

Petrography and bulk-rock geochemistry

Petrography. Samples from the CBB are represented by a wide group of very fine-grained sedimentary rocks such as sandstones, silty sandstones, siltstones and mudstones. Only sandstones and silty sandstones were taken into account for further investigations. In general, the mean grain size (Mz) of the sandstones falls in the very fine to fine sand fraction. Sorting is varied, from moderately well to very poorly sorted (Appendix 1). Lithoclasts are the most frequent among the framework elements (Appendix 1; Text-fig. 4). They are mainly of crystalline rocks, and plutonic fragments predominate. The plutonic lithoclasts recognised are dominated by granite. A few clasts of gabbro have also been noted. Volcanic lithics are present in one sample (outcrop 1085). Overall, metamorphic rock fragments were noted. They are represented by schists and a few rocks with a gneissic structure. Lithoclasts of sedimentary rocks are rarely present, and siltstones and cherts have been recognised in this group. Quartz is also an important component in the framework composition. Monocrystalline quartz is the most common. Feldspars were also noted. Micas, opaque minerals, heavy minerals and organic matter were observed only in trace amounts. The average framework composition of sandstones is Q40F10L50. The matrix content is high, with the exception of one sample (outcrop 877). The sandstones have been classified as feldspathic lithwackes, lithwackes and litharenites (Text-fig. 5A). Clay minerals and iron oxides/hydroxides were recognised as the most common diagenetic minerals. Moreover, porosity is changeable, from very low to high (c. 2–20%).

Bulk-rock geochemistry: major elements and geochemical classification (Appendix 2). The most abundant component in the CBB samples is SiO_2. The silica source is that of quartz grains and crystalline lithic grains. Na_2O and K_2O contents are very low, with Na_2O related to plagioclase and K_2O to K-feldspar. Strong positive correlation of K_2O and positive correlation of Na_2O with Al_2O_3 suggests accumulation of these elements among the finest fraction as clay minerals being an effect of weathering of feldspars. Al_2O_3 and CaO contents are low. Other oxides such as Fe_2O_3, MgO, TiO_2, P_2O_5 and MnO comprise only low or trace amounts in the samples.

The diagram for geochemical classification of sandstones (Herron 1988) was used in order to further classify the studied deposits (Text-fig. 5B). Samples from the CBB are classified as sublitharenites, litharenites and arkoses. Generally, the distribution of

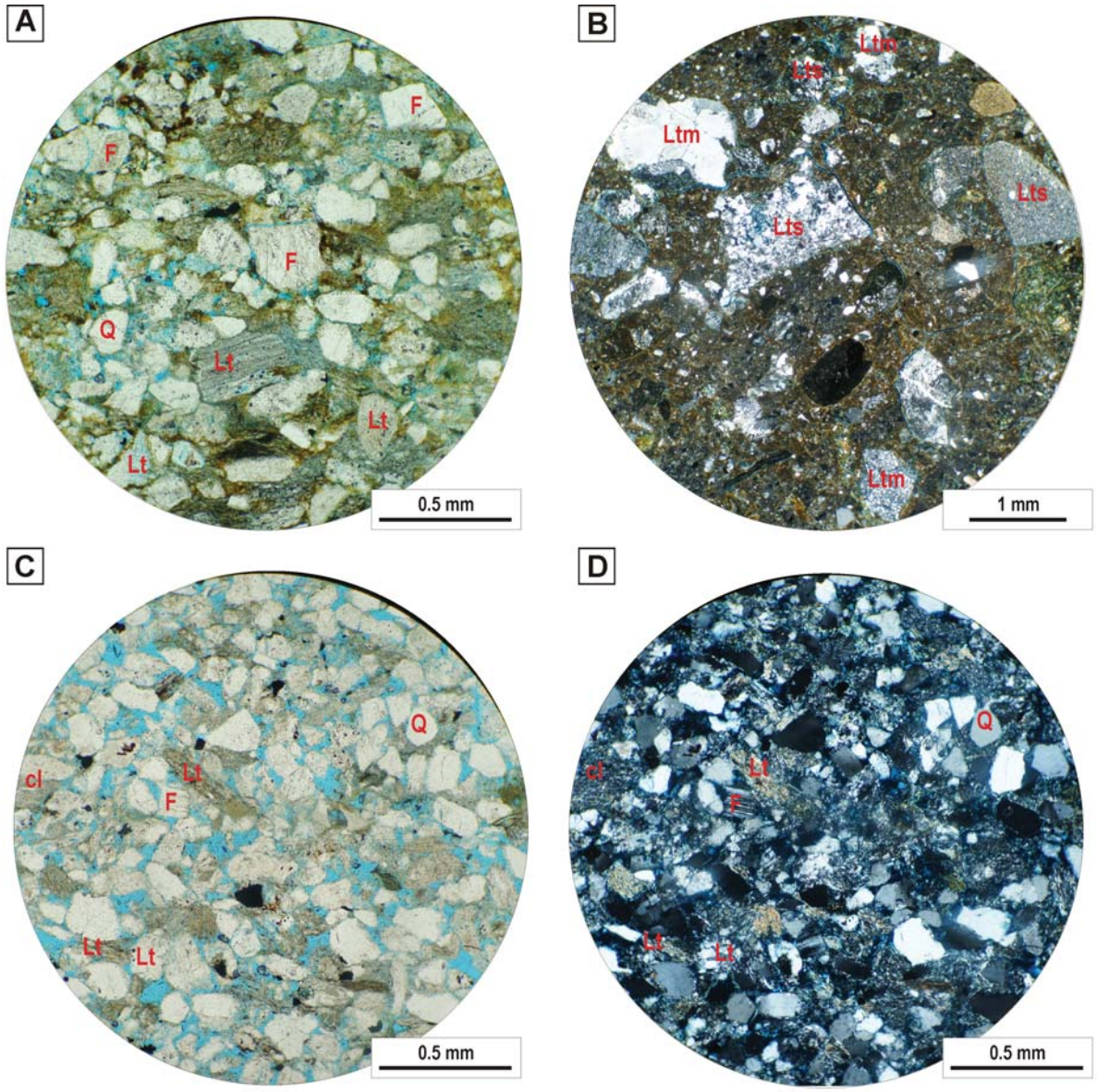

Text-fig. 4. Petrofacies distinguished in the CBB deposits. A – very fine to fine-grained moderately sorted lithwacke, sample CB6, outcrop 1073 (Lt – lithoclasts, F – feldspars, Q – quartz); porosity marked by blue epoxy; B – coarse-grained, very poorly sorted lithwacke, sample CB11, outcrop 1085 (Ltm – lithoclasts of magmatic felsic rocks, Lts – lithoclasts of fine grained sedimentary rocks); C, D – fine-grained moderately well sorted litharenite, sample CB13, outcrop 877 (Lt – lithoclasts, F – feldspars, Q – quartz, cl – clay minerals); porosity marked by blue epoxy. Plane-polarized light: A, C; cross-polarized light: B, D

oxides of major elements supports the mineralogical composition of the studied samples and confirms the results of the petrographic analysis.

Discussion. The source rock composition may be estimated based on petrographic results, i.e., types of lithoclasts distinguished in the studied samples, which are a reflection of palaeogeography. Sandstones from the CBB can be described as submature or even immature in a few cases. They contain a lot of lithoclasts, the composition of which depends on the sample location within the basin, e.g., in the middle of the basin the number of lithoclasts is the lowest, and they are represented by crystalline rock fragments which are difficult to recognise. Further southward the lithoclast content increases and the wide group

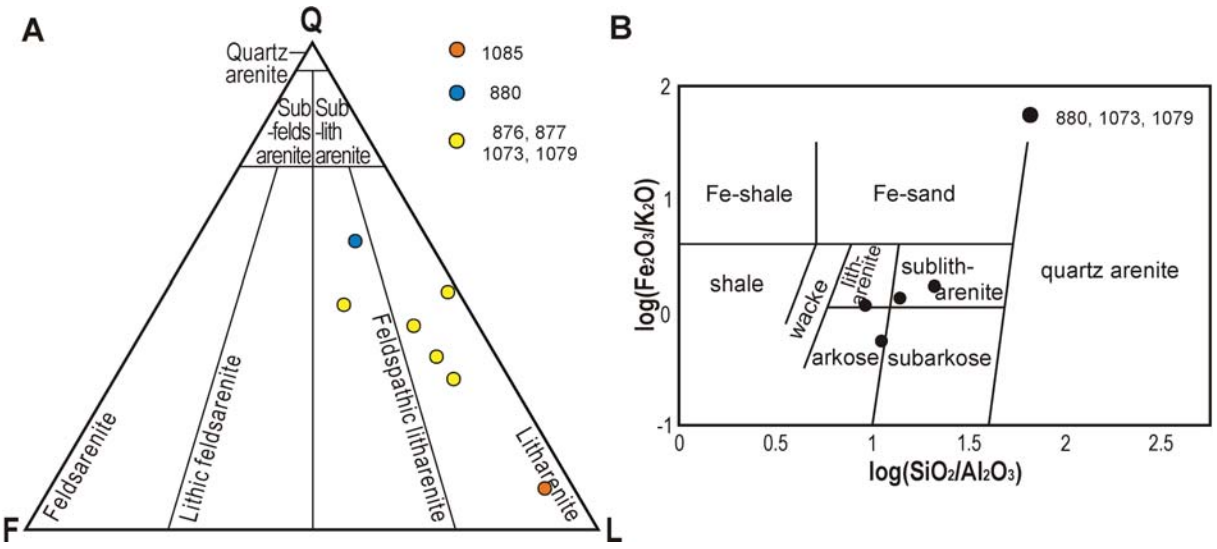

Text-fig. 5. A – Petrographic classification of sandstones in the QFL triangular diagram (diagram compiled and modified after: McBride 1963; Dott Jr. 1964; Folk *et al*. 1970; Pettijohn *et al*. 1972; Williams *et al*. 1982). Q – quartz, F – feldspars, L – lithoclasts. B – Geochemical classification of the studied sandstones (diagram after Herron 1988)

of lithoclasts is represented mostly by fragments of plutonic rocks, coupled with a low admixture of metamorphic and sedimentary rocks. In the SW and W parts of the basin the composition of the lithoclasts is similar, but within the sedimentary rock a few fragments of chert have been recognised. A different composition is observed in a sample from the NE part of the basin: it contains a lot of fragments of granitic rocks, very often with a well preserved myrmekite structure. There is also a group of volcanic lithoclasts (basalts?) followed by a few sedimentary rock fragments.

The potential source area was most likely composed of older sedimentary units, but the sample from outcrop 1079 (for location see Text-fig. 2) points to a change in the source composition, which could be related to the appearance of granitic rocks in the source. This change may be related with tectonic uplift of the area with a granitic massif located to the SW of the basin. The studied geochemical samples reflect a geochemical composition of silicic source rocks with only a minor contribution of basic components. Therefore, in general, derivation from areas located to the NE and NW of the basin is unlikely (Triassic gabbro and peridotite being present here), with exception of the most NE marginal part of the basin (outcrop 1085), where a small influx of a mafic component is expressed by the presence of a few lithic grains of gabbro and basalt.

Facies pattern

The clastic deposits filling the CBB represent alluvial fan, gravel-dominated fluvial channel, sand-dominated, flood plain/lake depositional environments (Text-figs 6 and 7; Table 1). The CBB was interpreted as the alluvial-fan to lacustrine basin (Wysocka 2009). Based on previous studies, two types of alluvial-fan conglomerates were distinguished (Wysocka 2009). The conglomerate beds of the first type are tabular, or broadly lenticular in shape, very poorly sorted, matrix- or clast-supported, with a variable coarse sand or mud matrix content. Quite often they contain several large, outsized cobbles and boulders (Text-fig. 6). The second type is represented by composite sequences of planar cross-bedded sand-supported conglomerates several metres thick, occasionally with sandstone alternations. The beds are usually sheet-like, with limited or insignificant basal erosion. They are composed of sand- and clast-supported, poor- to well-sorted, sub- to well-rounded pebble- to cobble-sized conglomerates. Other widely spread lithofacies are conglomerates and sandstones of the gravel-dominated fluvial channel depositional environment (Text-figs 6 and 7; Table 1). These are predominantly composed of planar and trough cross-stratified sand-supported conglomerates (Gp/Gt) and planar and trough cross-stratified sandstone (Sp/St) lithofacies, sub-

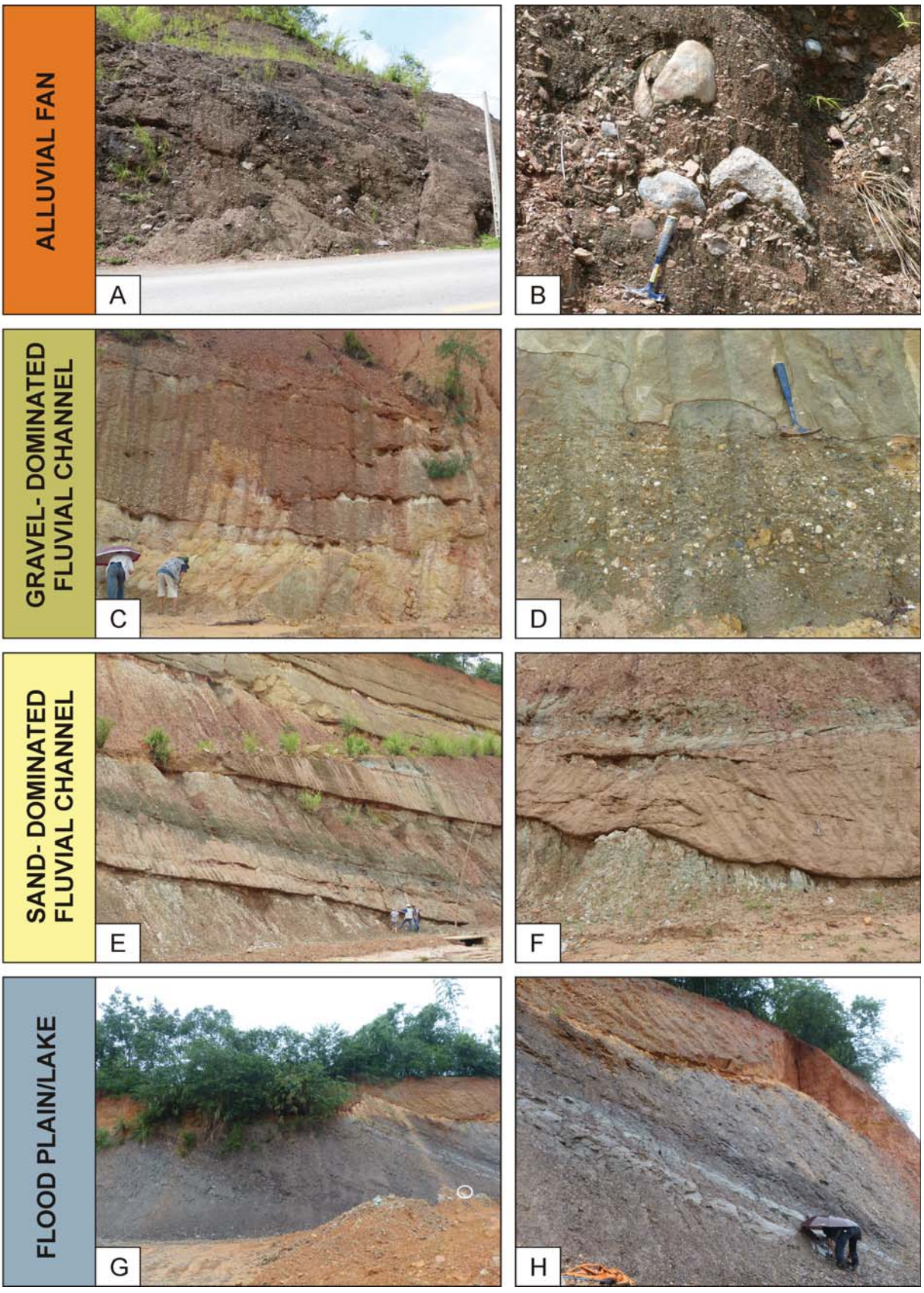
ALLUVIAL FAN
A
B
GRAVEL- DOMINATED FLUVIAL CHANNEL
C
D
SAND- DOMINATED FLUVIAL CHANNEL
E
F
FLOOD PLAIN/LAKE
G
H

ordinately with massive or amalgamated bodies of conglomerate (Gmm), massive or amalgamated beds of sandstone (Sm) and massive siltstone (Fsm) lithofacies. Texturally, they are built of sand- and clast-supported, poor- to well-sorted, sub-rounded to well-rounded pebble-to-cobble conglomerates, and poorly sorted pebbly sandstones. Sets of beds commonly have erosive bases and are sometimes amalgamated (Text-fig. 6). They are followed by more sandy lithofacies interpreted as being deposited in the sand-dominated fluvial channel depositional environment. As a rule, they show a fining-up trend in the topmost part of particular beds. The sets of beds are bound by distinct erosive surfaces and build thick bodies of channelized form cut in massive siltstones (Text-figs 6 and 7; Table 1). Sometimes trough cross-stratification is observed. The finest lithofacies are represented by fine-grained horizontally or ripple laminated sandstones. The reddish siltstones are typical of the flood plain depositional environment, whereas the fine-grained sequence dominated by grey clayey and silty deposits is interpreted as having been deposited in a lake environment (for details see Wysocka 2009).

Discussion. New investigations allow us to slightly change our previous interpretations of the facies pattern in the CCB fill. The first change concerns the sandy facies. Because of the fresh, unweathered cuts of new roads under construction it was possible to follow the facies changes in detail. This allowed us to prepare a new cross-section across the basin (Text-fig. 7A). We observed that the extent of the sandy facies in Wysocka (2009)was too narrow. Therefore, we decided to distinguish a sand-dominated fluvial channel facies in place of facies association V – lake margin/or river mouth of Wysocka (2009; compare Table 1 with table 2 in Wysocka 2009).

The second change is the reinterpretation of the conglomerates from the CBB. The coarse-grained facies crops out along the W, SE and E basin margins (see Wysocka 2009, fig. 5). However, the previously mentioned conglomerates of type 1 build the southernmost part of the basin whereas the conglomerates of type 1 and 2 build the continuous succession of the W basin margin. They are polymictic, characterised by diversified metamorphic and sedimentary lithoclasts, typically with white quartz pebbles. The sequence is fining-upward from the west to the basin centre and the conglomerates are interlayered with sand- and clast-supported, poor- to well-sorted, sub-rounded to well-rounded pebble-to-cobble conglomerates, and poorly sorted pebbly sandstones of the gravel-dominated fluvial channel facies (Text-figs 6 and 7). The general fining-upward trend continues through the sand-dominated fluvial channel facies and is followed by flood plain and lake facies (Text-fig. 7A).

Because of the high fluvial-lacustrine deposit thickness it is possible that this depositional system was a long-lasting type. Moreover, the lacustrine deposits from which the palynoflora was studied had been deposited in the upper part of the fluvial lacustrine system. This suggests that the Cao Bang deposits are of Eocene–Oligocene age.

Despite some faults cutting the sedimentary succession and the gradual dip increase, the succession could be treated as a fill typical of long-lasting evolving half-graben or strike-slip basins (Crowell and Link 1982; Mclaughlin and Nilsen 1982; Nilsen and Sylvester 1995; Porębski 1997; Ryang and Chough 1999; Gawthorpe and Leeder 2000; Kim *et al.* 2003). This is in good agreement with the petrographic and geochemical characteristics of these systems, which point to the source rock area being dominated by sedimentary rocks with a small amount of granitic rocks in the upper part of the sequence. Such a granite admixture may be related to tectonic uplift of the area with the granitic massif located somewhere to the south-west of the basin. The textural immaturity of this sequence points to short-distance, gravity-dominated transport from the source area for the alluvial facies (perpendicular to the basin extent) combined with relatively long-distance transport, of axial type, for the fluvial facies. Such a facies pattern suggests that the basin was bordered to the west by a high-relief hilly area. A similar facies pattern occurs in the southernmost tip of the basin as well (see fig. 5 in Wysocka 2009), however there the sedimentary dip of the conglomerate bodies is to the north-west.

← Text-fig. 6. Schematic sections for the interpreted depositional environments, general view (on the left) and close-up (on the right); see Table 1 for lithofacies code and details; see Text-fig. 2 for outcrop location. A, B – Alluvial fan – a body of highly amalgamated, cobble-to-pebble size conglomerates (Gmm), outcrop 1066; C, D – Gravel-dominated fluvial channel – a body of stacking, highly amalgamated, crudely or planar and low angle trough cross-stratified pebble-to-cobble size conglomerates with partly open-work fabric and fining-up trend (Gmg, Gp/Gt), outcrop 1079; E, F – Sand-dominated fluvial channel – a body of stacking, channelized, poorly sorted medium-to-coarse grained planar and trough cross-stratified sandstones cut in massive siltstones (Sp/St, Sm, Fsm), outcrop 876; G, H – Flood plain/lake – a thick section of coaly claystones and laminated siltstones (FC, Fl), tectonically tilted to the N, outcrop 1081, orange material circled on G is well visible on the down, right corner of H

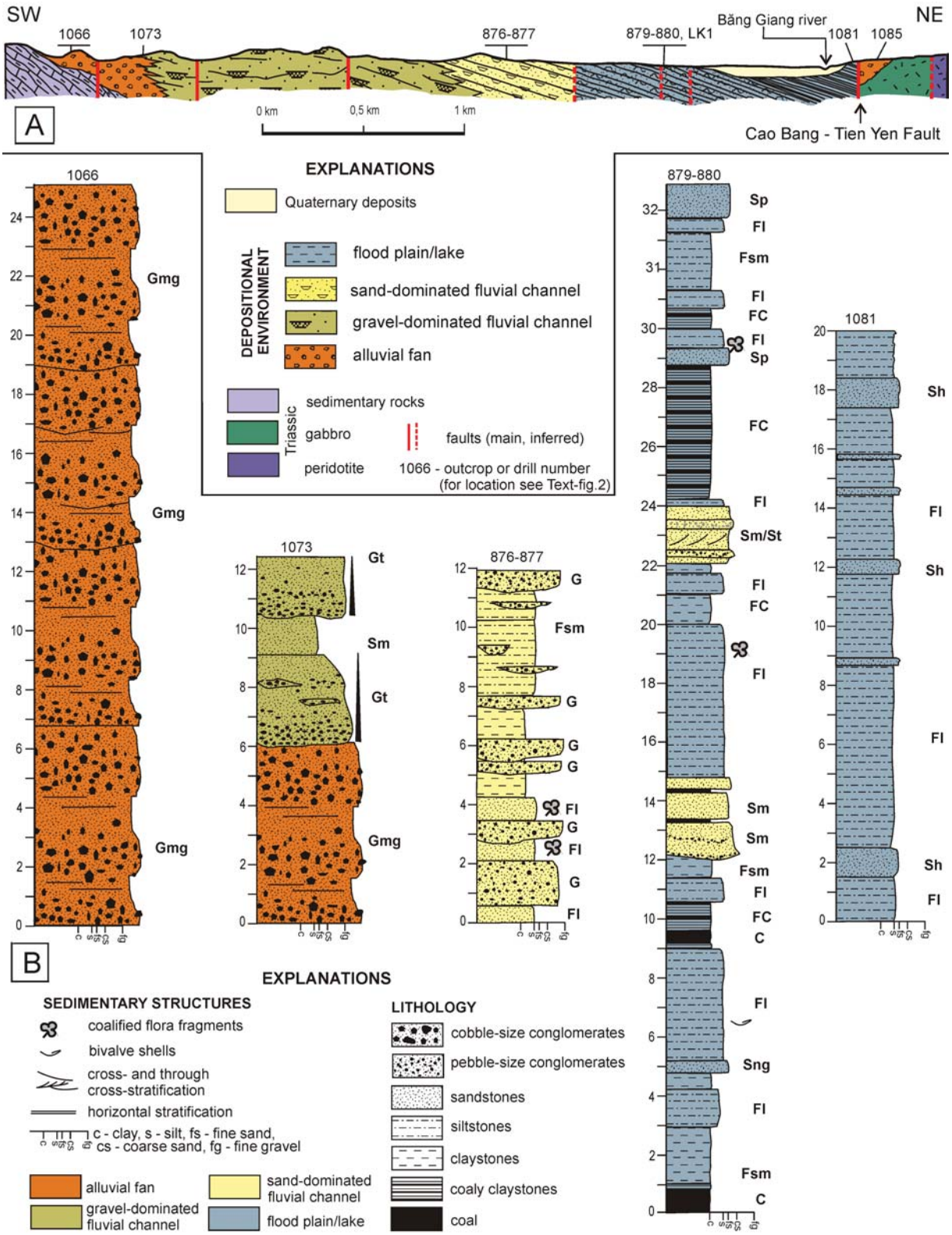

Text-fig. 7. A – Facies pattern of the Cao Bang Basin along the SW-NE cross-section line, based on field studies and interpretation of published geological maps (Cuong *et al*. 2000; Thuy 2000; Binh *et al*. 2003; Hoang *et al*. 2004; Hung *et al*. 2007 and Lan *et al*. 2011); B – Typical sections for the distinguished depositional environments of the Cao Bang Basin (based on Wysocka 2009)

Text-fig. 8. Characteristics of rocks from the north-eastern and eastern sides of the basin. Basement – mafic rocks: A – road cut about 1 km to the NE from outcrop 1085; B – road side about 200 m to the northeast from outcrop 1085, hammer is c. 30 cm long. Debris-flow dominated alluvial fan (outcrop 1085): C – contact between basement rocks (b) and breccias/conglomerates of the alluvial fan (af) outcrops of mafic rocks, * enlarged in E; ** enlarged in F. D – massive, monomictic, clast-supported breccia. Details of the contact between the basement rocks and the alluvial fan facies: E, F – tectonic breccia with slickensides

A different situation occurs on the opposite, eastern side of the CBB (in the line of the cross section – see Text-fig. 7A). Here, only a very narrow zone of breccias/conglomerates occurs. They are bordered from the northeast and east by basement rocks (Text-fig. 8A–C), i.e., Triassic gabbro and peridotite. From the southwest and south they are cut by a sharp tectonic contact with the finest facies of the CBB (Text-fig. 7A). The conglomerates are massive or crudely stratified, very poorly sorted, cobble-to-boulder-

sized, angular-to-sub-rounded with a variable matrix content (Text-fig. 8C, D). The clasts are represented only by mafic gabbroid-type rock fragments. They are interpreted as very proximal debris-flow deposits or even tectonic breccias, and should be treated as the third type of the Cao Bang conglomerates. The contact with the basement mafic Triassic rocks is sharp and strongly tectonized with numerous slickensides (Text-fig. 8E) and tectonic breccias (Text-fig. 8F). The slickensides point to the oblique-slip sense of movement. Detailed structural measurements and interpretations are needed for more conclusive results.

CONCLUSIONS

In response to newly published data on the CB-TY FZ and related basins, the Cao Bang Basin was revisited after more than 10 years. Based on our new studies we suggest that:

1. The previously accepted Miocene age of the CBB by Wysocka (2009) does not seem to be plausible in the light of our palynologic interpretations. Among the most frequent palynofloras of the CBB are saccate grains of gymnosperms, mainly of *Cathaya* and *Pinus*. *Carya*, *Celtis*, the Hammamelidaceae, *Ulmus* and also *Pterocarya*, *Quercus*, the *Castanea–Castanopsis–Lithocarpus* group, and the Loranthaceae prevailing among the angiosperms. The pteridophytes *Laevigatosporites*, Osmundaceae, and *Pteris* occur frequently in some samples. Most of the recognised taxa indicate a warm-temperate climate. The composition of the assemblage corresponds well with the lower part of the lower Oligocene PC1 complex of the Shangcun Formation from southern China. This statement is in good agreement with the revision of Böhme *et al.* (2011), in which the deposits from the Cao Bang Basin were ascribed to the lower Oligocene.

2. Sandstones from the CBB are submature or even immature in a few cases. They contain a lot of lithoclasts, the composition of which depends on the sample location within the basin. In the centre of the basin the number of lithoclasts is the lowest, and they are represented by crystalline rock fragments. Further southward, the lithoclast content increases and they are represented by plutonic rock fragments with a low admixture of metamorphic and sedimentary rocks. A different composition is observed in the north-easternmost marginal part of the basin. It contains a lot of granitic rocks fragments, very often with a well preserved myrmekite structure. There is also a group of volcanic lithoclasts (basalts?) followed by a few sedimentary rock fragments.

The potential source area was built of older sedimentary units and granitic rocks. The studied geochemical samples reflect a silicic source rock geochemical composition with only a minor contribution of the basic component. Therefore, in general, the derivation from areas located to the southwest and southeast of the basin was possible. The exception is the north-easternmost marginal part of the basin, where the influx of the mafic component is expressed by the presence of lithic grains of gabbro and basalt.

3. A sand-dominated fluvial channel facies has been distinguished in place of the facies association V – lake margin/or river mouth of Wysocka (2009). The textural immaturity of the CBB infill points to the short-distance, gravity-dominated transport from the source area for the alluvial facies (perpendicular to the basin extent) combined with the relatively long-distance transport, of axial type, for the fluvial facies. Moreover, the north-eastern margin is characterised by conglomerates built of mafic gabbroid-type rock fragments. These are interpreted as very proximal debris-flow deposits or even tectonic breccias. The succession that fills the CBB is interpreted as a fill typical of relatively long-lasting evolving half-graben or strike-slip basins.

4. The results mentioned can be combined with new data on the structural evolution of the area related to the Gulf of Tonkin (compare e.g., Fyhn and Phach 2015; Fyhn *et al.* 2018). Therefore, the CBB origin can be interpreted as being related to the later Eocene to late Oligocene transtensional rifting phase in the offshore Song Hong and Beibuwan basins. However, there are still some key regional questions such as: was the CBB linked with other basins (e.g., the Na Duong Basin) in one fluvial tract or not?; are the basins of the CB-TY FZ of the same age as those related to the Red River Fault Zone?; is the CBB offset from its primary position?; and were the basins related to the CB-TY FZ inverted and exhumed at the end of the Palaeogene as suggested by Fyhn *et al.* (2018) for the basins related to the Red River Fault Zone?

Acknowledgements

Warmest thanks are offered to Madelaine Böhme (University of Tübingen) and Peter Clift (Louisiana State University), the journal referees, for constructive comments and critical remarks which enabled the improvement of this paper. The fieldwork and analyses were financially supported by grants: VAST05.02/17-18 and QTPL01.02/18-19 (Vietnam) both to Dr. Phan Dong Pha, as well as partly by the Faculty of Geology, University of Warsaw (Poland).

REFERENCES

Alexandrova, G.N., Kodrul, T.M. and Jin, J.H. 2015. Palynological and paleobotanical investigations of Paleogene Sections in the Maoming Basin, South China. *Stratigraphy and Geological Correlation*, **23**, 300–325.

Allen, C.R., Gillespie, A.R., Han, Y., Sieh, K.E., Zhun, B. and Zhu, Ch.N. 1984. Red River and associated faults, Yunnan Province, China: Quaternary geology, slip rates, and seismic hazard. *Geological Society of America Bulletin*, **95**, 686–700.

Binh, N.B. (Ed.), Chau, N.N., Dien, N.V., Dat, P.M., Hoa, N.B. and Lai, N.Q. 2003. Geological Map of Cao Bang's Sheet. Scale: 1/ 25 000. In: Report on Geological Survey of Cao Bang-Ha Giang-Tuyen Quang Urbans (Cao Bang Urban). Union of Hydrogeology and Engineering Geology of Northern Vietnam, 187 p. Department of Geology and Mineral of Vietnam; Hanoi. [In Vietnamese]

Böhme, M., Aiglstorfer, M., Antoine P.-O., Appel, E., Havlik, P., Métais, G., Phuc, L.T., Schneider, S., Setzer, F., Tappert, R., Tran, D.N., Uhl, D. and Prieto, J. 2013. Na Duong (northern Vietnam) – an exceptional window into Eocene ecosystems from Southeast Asia. *Zitteliana A*, **53**, 120–167.

Böhme, M., Prieto, J., Schneider, S., Hung, N.V., Quang, D.D. and Tran, D.N. 2011. The Cenozoic on-shore basins of Northern Vietnam: Biostratigraphy, vertebrate and invertebrate faunas. *Journal of Asian Earth Sciences*, **40**, 672–687.

Chinh, V.V. 2000. Neotectonic evolution and mechanism of Cao Bang-Tien Yen Fault. *Journal of Sciences of the Earth*, **22**, 181–187.

Crowell, J.C. and Link, M.H. 1982. Geologic History of Ridge Basin, Southern California, 304 p. Field Trip Guidebook. Society of Economic Paleontologists and Mineralogists; Dallas, TX, Pacific Section.

Cuong, N.Q., Świerczewska, A., Wysocka, A., Pha P.D. and Huyen, V.N. 2006. Activity of the Cao Bang-Tien Yen Fault Zone (NE Vietnam) – record in associated sedimentary basins (P-074). Abstracts of the 17th International Sedimentological Congress, 21/8-7/9/2006, Fukuoka, Japan, vol. A, 290.

Cuong, N.T. (Ed.), Duc, L.V., Huy, D.Q., Khoa, H.V., Hoa, T.T. and Phong, N.V. 2000. Geological and mineral resources map of Cao Bang-Dong Khe Sheet. Scale: 1:50 000. Northeastern Geological Division. Department of Geology and Mineral of Vietnam; Hanoi. [In Vietnamese]

Dott, R.H., Jr. 1964. Wacke, greywacke, and matrix – what approach to immature sandstone classification? *Journal of Sedimentary Petrology*, **34**, 625–632.

Ducrocq, S., Benammi, M., Chavasseau, O., Chaimanee, Y., Suraprasit, K., Pha, P.D., Phuong, V.L., Phach, P.V. and Jaeger, J.-J. 2015. New anthracotheres (Cetartiodactyla, Mammalia) from the Paleogene of northeastern Vietnam: biochronological implications. *Journal of Vertebrate Paleontology*, **35**, e929139 (11 p.).

Folk, R.L., Andrews, P.B. and Lewis, D.W. 1970. Detrital sedimentary rock classification and nomenclature for use in New Zealand. *New Zealand Journal of Geology and Geophysics*, **13**, 937–968.

Fyhn, M.B.W. and Phach, P.V. 2015. Late Neogene structural inversion around the northern Gulf of Tonkin, Vietnam: Effects from right-lateral displacement across the Red River fault zone. *Tectonics*, **33**, 290–312.

Fyhn, M.B.W., Cuong, T.D., Hoang B.H., Hovikoski, J., Olivarius, M., Tuan, N.Q., Tung, N.T., Huyen, N.T., Cuong, T.X., Nytoft, H.P., Abatzis, I. and Nielsen, L.H. 2018. Linking Paleogene rifting and inversion in the northern Song Hong and Beibuwan basins, Vietnam, with left-lateral motion on the Ailao Shan-Red River Shear Zone. *Tectonics*, **37**, 2559–2585.

Gawthorpe, R.L. and Leeder, M.R. 2000. Tectono-sedimentary evolution of active extensional basins. *Basin Research*, **12**, 195–218.

Gmur, D., Świerczewska, A. and Wysocka, A. 2006. Depositional environment of Tertiary coals from Na Duong Basin Northern Vietnam. *Geoscientic Colloquium Reports*, **1**, 31–32.

Herman, A.B., Spicer, R.A., Aleksandrova, G.N., Yangd, J., Kodrul, T.M., Maslova, N.P., Spicer, T.E.V., Chen, G. and Jin, J.-H. 2017. Eocene–early Oligocene climate and vegetation change in southern China: Evidence from the Maoming Basin. *Palaeogeography*, *Palaeoclimatology*, *Palaeoecology*, **479**, 126–137.

Herron, M.M. 1988. Geochemical classification of terrigenous sands and shales from core or log data. *Journal of Sedimentary Petrology*, **58**, 820–829.

Hoang, T.N., Nguyen, V.H. and Nguyen, D.M. 2004. Na Rua-Cao Bang iron ore exploration project. Map no 1. General Department of Geology and Minerals of Vietnam; Hanoi. [In Vietnamese]

Hung, N.V. (Ed.), Hai, D.V., Van, T.V., Thao, N.T.P. and Viet, H.D. 2007. Report of project: Na Rua iron ore exploration in Tan Giang Ward, Cao Bang Town, Cao Bang Province. Northeast Vietnam Geological Division. Department of Geology and Mineral of Vietnam; Hanoi, 90 p. (Unpublished report) [In Vietnamese]

Ibrahim, A.C. 1933. Sporenformen des Aegirhorizonts des Ruhr-Reviers, 46 p. Buchdruckerei Konrad Triltsch; Würzburg.

Kim, S.B., Chough, S.K. and Chun, S.S. 2003. Tectonic controls on spatio-temporal development of depositional systems and generation of fining-upward basin fills in a strike-slip setting: Kyokpori Formation (Cretaceous), south-west Korea. *Sedimentology*, **50**, 639–665.

Krutzsch, W. 1959. Mikropaläontologische (sporenpaläontologische) Untersuchungen in der Braunkohle des Geiseltales. *Geologie*, **8**, 1–245.

Krutzsch, W. 1962. Stratigraphisch bzw. botanisch wichtige neue Sporen- und Pollenformen aus dem deutschen Tertiär. *Geologie*, **11**, 265–308.

Krutzsch, W. 1971. Atlas der mittel- und jungtertiären dispersen Sporen- und Pollen- sowie der Mikroplanktonformen des nördlichen Mitteleuropas. Lieferung VI, 234 p. VEB Gustav Fischer Verlag; Jena.

Lan, V.Q. (Ed.), Dung, N.T., Duong, T.B., Diep, C.X., Nang, N.V., Quyet, D.D., Quyet, H.B., Tai, V.D., Tien, B.C., Trung, N.H. and Uy, P.Q. 2011. Geological and Mineral Resources Map of Ha Quang's Sheet. Scale: 1:50 000. Northeastern Geological Division. Department of Geology and Mineral of Vietnam; Hanoi. [In Vietnamese]

Leloup, P.H., Arnaud, N., Lacassin, R., Kienast, J.-R., Harrison, T.M., Phan Trong, T.T., Replumaz, A. and Tapponnier, P. 2001. New constraints on the structure, thermochronology, and timing of the Ailao Shan-red River shear zone, SE Asian. *Journal of Geophysical Researches*, **106**, 6683–6732.

Leloup, P.H., Lacassin, R., Tapponnier, P., Schärer, U., Dalai, Z., Xiaohan, L., Liangshang, Z. and Trinh, P.T. 1995. The Ailao Shan-Red River shear zone (Yunnan, China), Tertiary transform boundary of Indochina. *Tectonophysics*, **251**, 3–84.

Longiaru, S. 1987. Visual comparators for estimating the degree of sorting from plane and thin section. *Journal of Sedimentary Petrology*, **57**, 791–794.

McBride, E.F. 1963. A classification of common sandstones. *Journal of Sedimentary Petrology*, **34**, 664–669.

McLaughlin, R.J. and Nilsen, T.H. 1982. Neogene non-marine sedimentation and tectonics in small pull-apart basins of the San Andreas fault system, Sonoma County, California. *Sedimentology*, **29**, 865–877.

Miall, A.D. 1977. A review of the braided river depositional environment. *Earth-Sciences Review*, **13**, 1–62.

Miall, A.D. 1978. Lithofacies types and vertical profile models in braided river deposits: a summary. In: Miall, A.D. (Ed.), Fluvial Sedimentology. *Canadian Society of Petroleum Geology Memoirs*, **5**, 597–604.

Morley, C.K. 2007. Variations in Late Cenozoic–Recent strike-slip and oblique-extensional geometries, within Indochina: The influence of pre-existing fabrics. *Journal of Structural Geology*, **29**, 36–58.

Morley, C.K. 2002. A tectonic model for the Tertiary evolution of strike-slip faults and rift basins in SE Asia. *Tectonophysics*, **347**, 189–215.

Nagy, E. 1969. Palynological elaborations of the Miocene layers of the Mecsek Mountains. *Annales Instituti Geologici Publici Hungarici*, **52**, 237–417.

Nakoman, E. 1965. Description d'un nouveau genre de forme: Corsinipollenites. *Annales de la Société Géologique du Nord*, **85**, 155–158.

Naumova, S.N. 1939. Spores and Pollen of the coals of the USSR. In: Report of the XVII International Geological Congress, Moscow 1937, vol. 1, pp. 355–366. Chief Editional Office of the mining-fuel and Geological Prospecting Literature; Moscow and Leningrad.

Neubauer, T.A., Schneider, S., Böhme, M. and Prieto, J. 2012. First records of freshwater rissooidean gastropods from the Palaeogene of southeast Asia. *Journal of Molluscan Studies*, **78**, 275–282.

Nhan, T.D. and Danh, T. 1975. New results of study on biostratigraphy of Neogene sediments of the NE Vietnam. In: Hao, D.X. (Ed.), Contribution of stratigraphy, pp. 244–283. Publish House of Science and Technology; Hanoi. [In Vietnamese]

Nilsen, T.H. and Sylvester, A.G. 1995. Strike-slip basins. In: Busby, C.J. and Ingersoll, R.V. (Eds), Tectonics of Sedimentary Basins, pp. 425–457. Blackwell; Cambridge.

Pettijohn, F.J., Potter, P.E. and Siever, R. 1972. Sand and Sandstones, 241 p. Springer-Verlag; New York.

Picard, M.D. 1971. Classification of fine-grained sedimentary rocks. *Journal of Sedimentary Petrology*, **41**, 179–195.

Pierce, R.L. 1961. Lower Upper Cretaceous plant microfossils from Minnesota. *Bulletin Geological Survey of University Minnesota*, **42**, 1–81.

Porębski, S. 1997. Slope-type fan delta in a strike-slip setting; Świebodzice Basin (Devonian–Carboniferous), Sudety Mts. In: Wojewoda, J. (Ed.), Obszary źródłowe: zapis kopalny, pp. 35–53. Wind; Wrocław. [In Polish]

Potonié, R. 1931. Zur Mikroskopie der braunkohlen Tertiäre Blütenstaubformen. I. *Braunkohle*, **30**, 325–333.

Potonié, R. 1934. Zur Mikrobotanik des eozänen Humodils des Geiseltales. *Arbeiten aus dem Institut für Paläobotanik und Petrographie der Brennsteine*, **4**, 25–125.

Potonié, R. 1951. Revision stratigraphisch wichtiger Sporomorphen des mitteleuropäischen Tertiärs. *Palaeontographica Abteilung B*, **91**, 131–151.

Potonié, R. 1956. Synopsis der Gattungen der Sporae dispersae I. *Beihefte zum Geologischen Jahrbuch*, **23**, 1–103.

Potonié, R. and Kremp, G. 1954. Die Gattungen der paläozoischen Sporae dispersae und ihre Stratigraphie. *Geologisches Jahrbuch*, **69**, 111–194.

Potonié, R., Thomson, P.W. and Thiergart, F. 1950. Zur Nomenklatur und Klassifikation der neogenen Sporomorphae. (Pollen und Sporen). *Geologisches Jahrbuch*, **65**, 35–70.

Prieto, J., Antoine, P.-O., van der Made, J., Métais, G., Phuc, L.T., Quan, Q.T., Schneider, S., Tran D.N., Vasilyan, D., Viet, L.T. and Böhme, M. 2018. Biochronological and palaeobiogeographical significance of the earliest Miocene mammal fauna from Northern Vietnam. *Palaeobiodiversity and Palaeoenvironments*, **98** (2), 287–313.

Pubellier, M., Rangin, C., Phach, P.V., Que, B.C., Hung, D.T. and Sang, C.L. 2003. The Cao Bang-Tien Yen Fault: Implications on the relationships between the Red River Fault and the South China Coastal Belt. *Advances in Natural Sciences*, **4**, 347–361.

Raatz, G.V. 1937. Mikrobotanisch-stratigraphische Untersuchung der Braunkohle des Muskauer Bogens. *Abhandlungen der Preussischen Geologischen Landesanstalt, Neue Folge*, **183**, 3–48.

Rangin, C., Klein, M., Roques, D., Le Pichon, X. and Trong,

L.V. 1995. The Red River fault system in the Tonkin Gulf, Vietnam. *Tectonophysics*, **243**, 209–222.

Ryang, W.H. and Chough, S.K. 1999. Alluvial-to-lacustrine systems in a pull-apart margin: southwestern Eumsung Basin (Cretaceous), Korea. *Sedimentary Geology*, **127**, 31–47.

Shaw, Ch.-L. 1998. Fossil Polygonaceous Palynomorphs of Taiwan. *Taiwania*, **43**, 27–32.

Spicer, R.A., Herman, A.B., Liao, W., Spicer, T.E.V. and Kordul, T.M. 2014. Cool tropics in the Middle Eocene: Evidence from the Changchang Flora, Hainan Island, China. *Palaeogeography*, *Palaeoclimatology*, *Palaeoecology*, **412**, 1–16.

Srivastava, S.K. 1966. Upper Cretaceous microflora, (Maastrichtian), from Scollard, Alberta, Canada. *Pollen et Spores*, **8**, 497–552.

Tapponnier, P., Lacassin, R., Leloup, P. H., Schärer, U., Dalai, Z., Xiaohan, L., Liangshang, Z. and Jiayou, Z. 1990. The Ailao Shan/Red River metamorphic belt: Tertiary left-lateral shear between Indochina and South China. *Nature*, **343**, 431–437.

Tapponnier, P., Peltzer, G. and Armijo, R. 1986. On the mechanics of the collision between India and Asia. In: Coward, M.P. and Ries, A.C. (Eds), Collision Tectonics. *Geological Society. Special Publication*, **19**, 115–157.

Taylor, S.R. and McLennan, S.M. 1985. The continental crust: its composition and evolution, 1–312. Blackwell Scientific Publications; Oxford.

Thomson, P.W. and Pflug, H. 1953. Pollen und Sporen des mitteleuropäischen Tertiärs. *Palaeontographica Abteilung B*, **94**, 1–158.

Thuan, D.V. 2006. Results of palynological analysis of the Neogene deposits from the northern part of Vietnam, 12 p. Vietnamese Academy of Science and Technology, Institute of Geological Sciences; Hanoi. (unpublished report) [In Vietnamese]

Thuy, D.K. 2000. Geological and mineral resources map of Lang Son Sheet. Scale: 1:200 000 (F-48-XXIII). Department of Geology and Mineral of Vietnam; Hanoi. [In Vietnamese]

Tri, T.V. and Khuc, V. 2011 (Eds). Geology and Earth Resources of Vietnam, 645 p. Publish House of Science and Technology; Hanoi. [In Vietnamese]

Trinh, D. 1979. Summary of hitherto research works on the paleontology and stratigraphy of the Tertiary sediments in the Vietnam territory. *PetroVietnam Review*, **143**, 10–12.

Trung, P.Q., Quynh, P.H., Bat, D., An, N.Q., Khoi, D.V. and Hieu, D.V. 2000. Database of Palynology (Spores and Pollens) of the Na Duong Formation. *PetroVietnam Review*, **7**, 18–27. [In Vietnamese]

Trung, P.Q., Quynh, P.H., Bat, D., An, N.Q., Khoi, D.V., Hieu, D.V. and Ngoc, N. 2000. New palynological investigation in the Na Duong mine. *Oil and Gas Journal* (Hanoi), **7**, 18–27.

Wang, 2006. Correlation of pollen sequences in the Neogene palynofloristic regions of China. *Palaeoworld*, **15**, 77–99.

Williams, H., Turner, F.J. and Gilbert C.M. 1982. Petrography, an introduction to the study of rocks in thin sections, 2nd ed., 626 p. W.H. Freeman & Co.; San Francisco.

Wodehouse, R.P. 1933. Tertiary Pollen. II. The oil shales the Eocene Green River Formation. *Bulletin of the Torrey Botanical Club*, **60**, 479–524.

Wolff, M. 1934. Mikrofossilien des pliozänen Humodils der Grube Freigericht bei Dettingen a. M. und Vergleich mit älteren Schichten des Tertiärs sowie posttertiären Ablagerungen. *Arbeiten aus dem Institut fur Paläobotanik und Petrographie der Brennsteine*, **5**, 55–95.

Wysocka, A. 2009. Sedimentary environments of the Neogene basins associated with the Cao Bang-Tien Yen Fault, NE Vietnam. *Acta Geologica Polonica*, **59**, 45–69.

Wysocka, A., Świerczewska, A., Cuong, N.C., Gmur, D., Phan, P.D. and Huyen, V.N. 2006. Depositional style of the Cao Bang-Tien Yen Fault Zone-related Neogene sedimentary basins (NE Vietnam) (O-328). Abstracts of the 17th International Sedimentological Congress, 21/8-7/9/2006, Fukuoka, Japan, vol. B, 209.

Wysocka, A., Świerczewska, A., Cuong, N.C., Gmur, D., Phan, D.P. and Huyen, V.N. 2005. Some remarks on the Neogene coal-bearing deposits from the Na Duong Basin (N Vietnam). Abstracts Volume, 8th International Conference on Fluvial Sedimentology, August 7–12, 2005, Delft, Netherlands, 318.

Yao, Y.-F., Bera, S., Ferguson, D.K., Mosbrugger, V., Khum, N., Jin, J.-H. and Li, Ch.-S. 2009. Reconstruction of paleovegetation and paleoclimate in the Early and Middle Eocene, Hainan Island, China. *Climatic Change*, **92**, 169–189.

Ye, Dequan, Zhong, Xiaochun, Yao, Yimin Yang, and Fan, Zhang Shiben. 1996. Tertiary in petroliferous regions of China, 375 p. Petroleum Industry Press; Beijing.

Yi, Sangheon, Yi, Songsuk, Batten, D.J., Yun, H. and Park, S.-J. 2003. Cretaceous and Cenozoic non-marine deposits of the Northern South Yellow Sea Basin, offshore western Korea: Palynostratigraphy and palaeoenvironments. *Palaeogeography, Palaeoclimatology*, *Palaeoecology*, **191**, 15–44.

Ziembińska-Tworzydło, M. 2009. *Cathayapollis* Ziembińska-Tworzydło gen. nov. In: Stuchlik, L. (Ed.), Atlas of pollen and spores of the Polish Neogene, Vol. 2, pp. 14–15. W. Szafer Institute of Botany, Polish Academy of Sciences; Kraków.

Manuscript submitted: 19th July 2018
Revised version accepted: 9th November 2018

Appendix 1. Point counting data and textural features of the studied samples

Sample		Framework components															
		Quartz						Q tot	Feld-spars	Lithoclasts							
		Qm nu	Qm u	Qp 2–3	Qp >3	Qm tot	Qp tot			Lt cryst nn	Lt cryst PL	Lt cryst MT	Lt cryst tot	Lt VL	Lt SED	Lt NN	Lt tot
877(17)1	CB13	19.00	0.00	6.00	1.00	19.00	7.00	26.00	7.00	5.00	13.00	4.00	22.00	0.00	2.00	5.00	29.00
876(17)1	CB12	18.00	0.00	2.00	0.00	18.00	2.00	20.00	6.00	15.00	3.00	3.00	21.00	0.00	5.00	4.00	30.00
1085(17)1	CB11	4.00	0.00	1.00	0.00	4.00	1.00	5.00	3.00	8.00	18.00	0.00	26.00	9.00	3.00	11.00	49.00
1079(17)2	CB10	17.00	2.00	6.00	1.00	19.00	7.00	26.00	12.00	3.00	5.00	0.00	8.00	0.00	3.00	7.00	18.00
1079(17)1	CB9	17.00	0.00	1.00	1.00	17.00	2.00	19.00	6.00	2.00	23.00	4.00	29.00	0.00	0.00	7.00	36.00
1073(17)1	CB6	13.00	4.00	6.00	3.00	17.00	9.00	26.00	1.00	8.00	8.00	1.00	17.00	0.00	6.00	3.00	26.00
880(17)4	CB4	21.00	1.00	6.00	0.00	22.00	6.00	28.00	6.00	10.00	2.00	0.00	12.00	0.00	0.00	1.00	13.00
Cao Bang Basin	min	4.00	0.00	1.00	0.00	4.00	1.00	5.00	1.00	2.00	2.00	0.00	8.00	0.00	0.00	1.00	13.00
	max	21.00	4.00	6.00	3.00	22.00	9.00	28.00	12.00	15.00	23.00	4.00	29.00	9.00	6.00	11.00	49.00
	avg	15.57	1.00	4.00	0.86	16.57	4.86	21.43	5.86	7.29	10.29	1.71	19.29	1.29	2.71	5.43	28.71

Sample		Others						∑ FC	Matrix	Cements/diagenetic minerals				∑ C	Porosity
		Micas	Opaque minerals	Organic matter	Heavy minerals	Bio-clasts	nn			Clay	Fe	Clay-Fe	Carbo-nate		
877(17)1	CB13	1.00	0.00	0.00	0.00	0.00	1.00	64.00	0.00	13.00	0.00	0.00	0.00	13.00	23.00
876(17)1	CB12	7.00	0.00	1.00	1.00	0.00	2.00	67.00	10.00	18.00	3.00	0.00	0.00	21.00	2.00
1085(17)1	CB11	0.00	0.00	0.00	0.00	0.00	6.00	63.00	28.00	6.00	0.00	1.00	0.00	7.00	2.00
1079(17)2	CB10	0.00	1.00	0.00	0.00	0.00	2.00	59.00	11.00	19.00	1.00	0.00	0.00	20.00	10.00
1079(17)1	CB9	2.00	1.00	0.00	0.00	0.00	1.00	65.00	8.00	23.00	0.00	0.00	0.00	23.00	4.00
1073(17)1	CB6	1.00	0.00	0.00	0.00	0.00	2.00	56.00	9.00	9.00	13.00	10.00	0.00	32.00	3.00
880(17)4	CB4	4.00	2.00	0.00	2.00	0.00	2.00	57.00	8.00	22.00	1.00	0.00	0.00	23.00	12.00
Cao Bang Basin	min	0.00	0.00	0.00	0.00	0.00	1.00	56.00	0.00	6.00	0.00	0.00	0.00	7.00	2.00
	max	7.00	2.00	1.00	2.00	0.00	6.00	67.00	28.00	23.00	13.00	10.00	0.00	32.00	23.00
	avg	2.14	0.57	0.14	0.43	0.00	2.29	61.57	10.57	15.71	2.57	1.57	0.00	19.86	8.00

Qm nu – monocrystalline nonundulatory quartz grains;
Qm u – monocrystalline undulatory quartz grains;
Qp 2-3 – polycrystalline quartz grains with 2–3 crystals per grain;
Qp >3 – polycrystalline quartz grains with more than 3 crystals per grain;
Qm tot – total amount of monocrystalline quartz;
Qp tot – total amount of polycrystalline quartz;
Q tot – total amount of quartz;
Lt cryst nn – lithoclasts of crystalline rocks difficult for unambiguous description;
Lt cryst PL – lithoclasts of plutonic rocks;
Lt cryst MT – lithoclasts of metamorphic rocks;
Lt cryst tot – total amount of lithoclasts of crystalline rocks;
Lt VL – lithoclasts of volcanic rocks;
Lt SED – lithoclasts of sedimentary rocks;
Lt NN – lithoclasts difficult for unombiguous classification;
Lt tot – total amount of lithoclasts;
nn – nonrecognisable framework components;
FC – framework components;
Fe – iron oxides/hydroxides;
C – cements/diagenetic minerals;
min – minimal value;
max – maximal value;
avg – average value

Appendix 2. Geochemical characteristics of the studied samples; values for UCC and PASS listed for comparison

ICP-ES [wt. %]														
		SiO_2	Al_2O_3	Fe_2O_3	MgO	CaO	Na_2O	K_2O	TiO_2	P_2O_5	MnO	Cr_2O_3	LOI#	Sum
	MDL	0.01	0.01	0.04	0.01	0.01	0.01	0.01	0.01	0.01	0.01	0.002	-5.1	0.01
Location	Sample													
880(17)4	CB 4	86.82	6.23	1.5	0.5	0.06	0.04	1.13	0.56	0.06	<0.01	0.006	3	99.92
880(17)5	CB 5	90.51	4.26	1.35	0.39	0.03	0.03	0.8	0.6	0.03	0.01	0.005	1.9	99.9
1073(17)1	CB 6	82.46	8.89	2.24	0.74	0.05	0.04	1.93	0.61	0.04	0.02	0.009	2.8	99.88
1079(17)2	CB 10	86.58	7.71	0.81	0.31	0.02	0.03	1.45	0.54	0.02	<0.01	0.007	2.4	99.93
UCC (Rudnick and Gao 2003)		66.55	15.39	5.04	2.48	3.59	3.27	2.80	0.64	0.15	0.10			100.00
PAAS (Taylor and McLennan 1985)		62.80	18.90	7.23	2.20	1.30	1.20	3.70	1.00	0.16	0.11			98.60

ICP-MS [ppm]												
		Ba	Be	Co	Cs	Ga	Hf	Nb	Rb	Sc	Sn	Sr
	MDL	1	1	0.2	0.1	0.5	0.1	0.1	0.1	1	1	0.5
Location	Sample											
880(17)4	CB 4	226	1	6.4	5.4	7.8	6.3	9.3	58.2	7	2	38.6
880(17)5	CB 5	131	1	15	3.4	5	10.5	9.4	39.6	5	1	13.6
1073(17)1	CB 6	317	<1	9.8	9.5	11.1	6.2	9.9	91	9	4	19.9
1079(17)2	CB 10	227	3	1.2	6.9	8	4.4	8.3	68.2	7	2	18
UCC (Rudnick and Gao 2003)		628.00		17.30	4.90	17.5	5.30	12.00	82.00	14.00	2.1	320.00
PAAS (Taylor and McLennan 1985)		650.00		23.00	15.00	20	5.00	19.00	160.00	16.00		200.00

ICP-MS [ppm]													
		Ta	Th	U	V	W	Zr	Y	La	Ce	Pr	Nd	Sm
	MDL	0.1	0.2	0.1	8	0.5	0.1	0.1	0.1	0.1	0.02	0.3	0.05
Location	Sample												
880(17)4	CB 4	0.7	8.6	2.2	64	2.1	256.1	17.6	29	55.7	6.17	22.5	3.87
880(17)5	CB 5	0.8	9.6	2.3	39	2	404.3	17.4	35.8	74.3	8.43	31.2	5.56
1073(17)1	CB 6	0.7	11.4	2.5	85	2.8	235.9	32	44.7	84.8	10.75	40	7.24
1079(17)2	CB 10	0.6	8.7	1.8	71	3	172.3	19	35.3	66.6	7.99	30.3	5.01
UCC (Rudnick and Gao 2003)		0.90	10.50	2.70	97.00	1.9	193.00	21.00	31.0	63.0	7.1	27.0	4.70
PAAS (Taylor and McLennan 1985)		1.50	14.60	3.10	150.00		210.00	27.00	38.2	79.6	8.8	33.9	5.55

ICP-MS [ppm]												
		Eu	Gd	Tb	Dy	Ho	Er	Tm	Yb	Lu	Mo	Cu
	MDL	0.02	0.05	0.01	0.05	0.02	0.03	0.01	0.05	0.01	0.1	0.1
Location	Sample											
880(17)4	CB 4	0.71	3.12	0.49	2.93	0.64	1.97	0.28	1.96	0.29	0.4	13
880(17)5	CB 5	0.85	4.1	0.56	3.19	0.61	1.89	0.26	1.79	0.3	0.3	14.2
1073(17)1	CB 6	1.35	6.44	0.96	5.32	1.15	3.2	0.44	2.61	0.42	0.2	38.2
1079(17)2	CB 10	0.94	4.07	0.58	3.36	0.7	1.9	0.27	1.9	0.27	0.3	6.1
UCC (Rudnick and Gao 2003)		1.00	4.00	0.70	3.90	0.83	2.30	0.30	2.00	0.31	1.1	28.00
PAAS (Taylor and McLennan 1985)		1.08	4.66	0.77	4.68	0.99	2.85	0.41	2.82	0.43	1	50.00

ICP-MS [ppm]												
		Zn	Ni	As	Cd	Sb	Bi	Ag	Au	Hg	Tl	Se
	MDL	1	0.1	0.5	0.1	0.1	0.1	0.1	0.5	0.01	0.1	0.5
Location	Sample											
880(17)4	CB 4	68	13.1	2.8	0.2	1.2	0.1	0.2	<0.5	0.05	<0.1	<0.5
880(17)5	CB 5	89	50	1.9	0.2	0.4	<0.1	<0.1	1.1	0.05	<0.1	<0.5
1073(17)1	CB 6	176	35.5	2.8	0.5	0.6	0.2	<0.1	1.4	0.07	0.1	<0.5
1079(17)2	CB 10	61	2.5	1.5	<0.1	0.5	0.1	<0.1	2.1	0.02	<0.1	<0.5
UCC (Rudnick and Gao 2003)		67.00	47.00	4.80	0.09	0.4	0.16	53		0.05	0.9	0.09
PAAS (Taylor and McLennan 1985)		85.00	55.00									

ICP-ES – Inductively Coupled Plasma – Emission Spectrometry;
ICP-MS – Inductively Coupled Plasma – Mass Spectrometry;
wt. % – Weight percent; ppm – Parts per million; ppb – Parts per billion;
MDL – Measurement detection limit;
LOI – Lost on ignition ($^{\#}$ by weight difference after ignition at 1000°C)